Published in final edited form as:

N Engl J Med. 2021 September 02; 385(10): 921–929. doi:10.1056/NEJMoa2102715.

Treatment of Relapsing HPV Diseases by Restored Function of Natural Killer Cells

Andrea Lisco, M.D., Ph.D.,
Laboratories of Immunoregulation, Bethesda, MD

Amy P. Hsu, B.S.,
Clinical Immunology and Microbiology, Bethesda, MD

Dimana Dimitrova, M.D.,
National Institute of Allergy and Infectious Diseases, the Experimental Transplantation and Immunotherapy Branch, Bethesda, MD

Diana M. Proctor, Ph.D.,
National Cancer Institute, the Translational and Functional Genomics Branch, National Human Genome Research Institute, Bethesda, MD

Emily M. Mace, Ph.D.,
Vagelos College of Physicians and Surgeons, Columbia University, New York

Peiying Ye, Ph.D.,
Laboratories of Immunoregulation, Bethesda, MD

Megan V. Anderson, R.N., B.A.,
Laboratories of Immunoregulation, Bethesda, MD

Stephanie N. Hicks, R.N., B.S.N.,
National Institute of Allergy and Infectious Diseases, the Experimental Transplantation and Immunotherapy Branch, Bethesda, MD

Christopher Grivas, B.S.,
Laboratories of Immunoregulation, Bethesda, MD

Dima A. Hammoud, M.D.,
Center for Infectious Disease Imaging, Bethesda, MD

Maura Manion, M.D.,
Laboratories of Immunoregulation, Bethesda, MD

Gabriel J. Starrett, Ph.D.,
Laboratory of Cellular Oncology, Bethesda, MD

Address reprint requests to Dr. Lisco at the Laboratory of Immunoregulation, National Institute of Allergy and Infectious Diseases, National Institutes of Health, 9000 Rockville Pike, Bldg. 10, Rm. 6D44G, Bethesda, MD 20892, or at andrea.lisco@nih.gov.
Drs. Hsu, Dimitrova, Proctor, and Mace contributed equally to this article.

Supported by the Intramural Research Programs of the National Institutes of Health (NIH) and by a grant (P30CA013696) from the Herbert Irving Comprehensive Cancer Center Flow Cytometry Shared Resources.
Disclosure forms provided by the authors are available with the full text of this article at NEJM.org.
A data sharing statement provided by the authors is available with the full text of this article at NEJM.org.

Alvin Farrel, Ph.D.,
Laboratory of Molecular Immunology and the Immunology Center, National Heart, Lung, and Blood Institute, Bethesda, MD

Kerry Dobbs, M.S.,
Clinical Immunology and Microbiology, Bethesda, MD

Isaac Brownell, M.D., Ph.D.,
Dermatology Branch, National Institute of Arthritis and Musculoskeletal and Skin Diseases, Bethesda, MD

Christopher Buck, Ph.D.,
Laboratory of Cellular Oncology, Bethesda, MD

Luigi D. Notarangelo, M.D.,
Clinical Immunology and Microbiology, Bethesda, MD

Jordan S. Orange, M.D., Ph.D.,
Vagelos College of Physicians and Surgeons, Columbia University, New York

Warren J. Leonard, M.D.,
Laboratory of Molecular Immunology and the Immunology Center, National Heart, Lung, and Blood Institute, Bethesda, MD

Michael I. Orestes, M.D.,
National Institutes of Health, and Walter Reed National Military Medical Center, Bethesda, MD

Anju T. Peters, M.D.,
Department of Medicine and Department of Otolaryngology-Head and Neck Surgery, Northwestern University Feinberg School of Medicine, Chicago

Jennifer A. Kanakry, M.D.,
National Institute of Allergy and Infectious Diseases, the Experimental Transplantation and Immunotherapy Branch, Bethesda, MD

Julia A. Segre, Ph.D.,
National Cancer Institute, the Translational and Functional Genomics Branch, National Human Genome Research Institute, Bethesda, MD

Heidi H. Kong, M.D.,
Dermatology Branch, National Institute of Arthritis and Musculoskeletal and Skin Diseases, Bethesda, MD

Irini Sereti, M.D., M.H.S.
Laboratories of Immunoregulation, Bethesda, MD

SUMMARY

Human papillomavirus (HPV) infections underlie a wide spectrum of both benign and malignant epithelial diseases. In this report, we describe the case of a young man who had encephalitis caused by herpes simplex virus during adolescence and currently presented with multiple recurrent skin and mucosal lesions caused by HPV. The patient was found to have a pathogenic germline

mutation in the X-linked interleukin-2 receptor subunit gamma gene (*IL2RG*), which was somatically reverted in T cells but not in natural killer (NK) cells. Allogeneic hematopoietic-cell transplantation led to restoration of NK cytotoxicity, with normalization of the skin microbiome and persistent remission of all HPV-related diseases. NK cytotoxicity appears to play a role in containing HPV colonization and the ensuing HPV-related hyperplastic or dysplastic lesions. (Funded by the National Institutes of Health and the Herbert Irving Comprehensive Cancer Center Flow Cytometry Shared Resources.)

HUMAN PAPILLOMAVIRUS (HPV) INFECTION CAUSES UP TO 4.5% OF ALL new cancer cases worldwide and represents 29.5% of all infection-related cancers. The immunologic determinants of HPV epithelial colonization, persistence, and progression to HPV-associated dysplasia are largely unknown. Thus, integrated and definitive immunologic therapies are not yet available. Although antibodies to the L1 major capsid protein of HPV are sufficient to prevent the infection of keratinocytes by the most common α-HPV genotypes,[1,2] more elaborate innate and adaptive immunologic functions appear to be required to prevent the development of incidental HPV-related hyperproliferative or dysplastic lesions after HPV infection of keratinocytes has occurred.[3–5]

The study of inborn errors of immunity can help decipher the role of specific immune functions in HPV immunopathogenesis. Here, we show that a novel pathogenic germline allele in the X-linked interleukin-2 receptor subunit gamma gene (*IL2RG*) underwent a somatic mutation resulting in reversion of the pathogenic allele in T cells but not in natural killer (NK) cells, with subsequent expansion of the HPV skin virome and recalcitrant HPV-related skin and mucosal diseases. The regression of both benign and malignant HPV-related lesions along with re-equilibration of the skin microbiome after the restoration of specific immunologic functions following hematopoietic-cell transplantation (HCT) illustrates the implications of integrated ablative and immunotherapeutic approaches to HPV-related diseases and contributes to defining the role of NK cells in host defense.

METHODS

A comprehensive description of the experimental methods that were used in this analysis is provided in the Materials section in the Supplementary Appendix, available with the full text of this article at NEJM.org, along with the clinical protocol, which was approved by the institutional review board at the National Institutes of Health. All the participants in this study, including the case patient who is described, provided written informed consent.

CASE REPORT

A 23-year-old Black man with a history of left temporal lobe herpes simplex virus (HSV) encephalitis during adolescence (Fig. S1A and S1B in the Supplementary Appendix) had numerous flat warts (verruca plana) on his scalp extending beyond the hairline and scattered verruca vulgaris on his face, limbs, and trunk in the absence of any anogenital lesion (Fig. S1C and S1D). He had a 5-year history of a nonhealing left nasal ulcer and was found to have a sessile, raised left nasal vestibular lesion (Fig. 1A). A biopsy revealed an HPV-related squamous-cell carcinoma in situ, with positive staining for the surrogate marker of high-risk

HPV, antibody against $p16^{INK4a}$, a protein that is involved in regulation of the cell cycle (Fig. 1B and 1C). HPV genotyping with the use of a clinical HPV-DNA hybridization assay of a biopsy sample obtained from the nasal vestibular lesion was negative for common low-risk and high-risk HPV variants, but more sensitive next-generation RNA sequencing revealed high-risk α-variant HPV-16 infection (Fig. S2).

Although the nasal mass was surgically debrided with clear margins, three subsequent recurrences of the squamous-cell carcinoma in the left nasal vestibule required further surgical resections. Partial rhinectomy with radiation therapy was proposed after the fourth recurrence, but concerns regarding disfiguring complications, further recurrence, and progression to invasive squamous-cell carcinoma prompted immunologic evaluation to inform a poentially less invasive and more effective integrated treatment.

Immunophenotyping of a peripheral-blood sample showed a modest decrease in the absolute number of CD4+ T cells (287 cells per cubic millimeter; reference range, 359 to 1656) and a large expansion of polyclonal CD3$\alpha\beta$+CD8+ cells (2907 cells per cubic millimeter; reference range, 178 to 853) of the prevalent phenotype of NK-like T cells (CD3$\alpha\beta$+CD8+CD56+CD57+) without evidence of increased expression of programmed cell death protein 1 (Fig. 2A, Table S1, and Figs. S3, S4, and S5). The absolute number of NK cells (181 cells per cubic millimeter; reference range, 126 to 729) and their degranulation function were preserved (Fig. S6). In contrast, a reduction in the number of NK cells that were functionally mature(CD3−$CD56^{dim}$CD16+) and terminally mature (KIR+), with relative expansion of immature NK cells (CD3−$CD56^{bright}$CD16−) and expansion of the skin-homing NK subset expressing the cutaneous lymphocyte-associated antigen, was observed (Figs. S4B and S6). Absolute levels of B cells and immunoglobulin M, A, and E were normal, whereas IgG levels were elevated. Diphtheria- and tetanus-specific antibody titers were protective (Table S1).

Whole-blood next-generation gene sequencing revealed a novel heterozygous missense transition — c.191T→C (p.V64A) — in *IL2RG*, which is mutated in humans with X-linked severe combined immunodeficiency.[6,7] The protein encoded by *IL2RG* is also known as the common cytokine receptor γ-chain, since it is shared by several interleukins (2, 4, 7, 9, 15, and 21).[6] Both mutated and wild-type alleles were similarly distributed in whole-blood DNA (Fig. 2B). No karyotypic abnormalities or copy-number variations were found in the cytogenetic analysis of bone marrow aspirate or peripheral blood to account for apparent heterozygosity for an X-linked allele. DNA sequencing of *IL2RG* in whole-blood samples obtained from the patient's mother, grandmother, and three female siblings showed heterozygous c.191T→C, whereas complementary DNA extracted from sorted cells of a heterozygous female sibling revealed only the wild-type allele (c.191T), a finding that was consistent with skewed X-inactivation due to the deleterious effect of c.191T→C on T-cell development (Fig. 2C and D).

IL2RG sequencing of the patient's CD34+ hematopoietic stem cells and sorted immune-cell population (CD4+ T cells, CD8+ T cells, CD3− CD56+CD16+ NK cells, CD14+ monocytes, and CD19+ B cells) documented the somatic reversion of the c.191T→C (p.V64A) germline variant in T cells (Fig. 2E). In genomic DNA extracted from CD34+

stem cells, only the mutant allele (c.191C) was detected. In contrast, CD3+CD8+ T cells and a large proportion of CD3+CD4+ T cells had the wild-type allele (c.191T), whereas other immune cells, including NK cells and monocytes, had evidence only of the mutated c.191C allele. The analysis of the distribution of wild-type and mutant alleles in CD4+ and CD8+ T-cell subsets confirmed the homogeneous selection of the *IL2RG* wild-type allele in CD4+ and CD8+ T-cell effector subsets, in regulatory T cells, and in NK-like CD8+ T cells, findings that were consistent with the requirement for functional signaling by the common cytokine receptor γ-chain for T-cell development, maturation, and differentiation (Figs. S7, S8, and S9A).

The evaluation of the biologic effects of p.V64A on the function of the common cytokine receptor γ-chain revealed that p.64V is conserved across species and is involved in stabilizing the helix-loop region in the cytokine binding site of the common cytokine receptor γ-chain (Fig. 2F). Accordingly, the missense variant V64A did not affect membrane expression (Fig. S9B), but intracellular signaling was impaired, as documented by the reduced level of phosphorylated signal transducer and activator of transcription 5 (pSTAT5) in response to interleukin-2 and interleukin-15 stimulation in mutant NK cells but not in somatically reverted CD4+ and CD8+ T cells (Fig. 2G and Fig. S10). Reduced expression of granzyme B and perforin with a resulting severe reduction in NK cytotoxic function was also documented (Fig. 3A and 3B). Such genetic and immunologic analyses confirmed the pathogenicity of V64A, which was masked in heterozygous female carriers by skewed X-inactivation and mitigated in the case patient by somatic reversion in a lymphoid precursor already committed to T-cell lineage development.

To investigate the effect of the NK functional defect on the clinical phenotype of the case patient, we performed shotgun metagenomic sequencing of the microbiome obtained from 10 sites on the patient's skin and oropharynx. We found a marked expansion in the relative abundance of the skin virome, particularly of HPVs, in stark contrast to that in healthy controls, who had bacterial preponderance and lower viral representation (Fig. 3C and Fig. S11). Moreover, skin was enriched in α-HPVs, the HPV genus most classically associated with HPV-related epithelial dysplasia, along with a higher relative abundance of β-HPVs and absence of γ-HPVs, a main component of the skin virome in healthy persons.[8]

TREATMENT

The severely impaired immunologic control of HPVs and the consequent increased risk of progression to invasive or metastatic disease of the multiply recurrent HPV-16–related nasal squamous-cell carcinomas required an integrated approach with ablative and immunologic treatment. In July 2017, we performed photodynamic laser ablation of the nasal HPV-16–related tumor to minimize the risk of progression during HCT. Then, in November 2017, the patient underwent reduced-intensity-conditioning HCT with a T-replete bone marrow graft from his sister who was a heterozygous *IL2RG* mutation carrier[9] with favorable skewed X-inactivation and who had human leukocyte antigens that matched her brother's antigens (Fig. 2D and the Methods section in the Supplementary Appendix).

The post-HCT course was uncomplicated, with the exception of self-limited BK virus–associated hemorrhagic cystitis. Full (>95%) donor myeloid and NK chimerism occurred rapidly within 60 days after HCT, whereas full donor T-cell and B-cell chimerism occurred within 6 months after HCT (Fig. S12). No recurrence of nasal dysplasia or squamous-cell carcinoma was observed 3 years after HCT, as documented by clinical examinations and combined positron-emission tomography and computed tomography with ^{18}F-fluorodeoxyglucose; a remarkable regression of skin verruca was also noted within 1 year after HCT (Fig. 1D through 1G and Fig. S1C through S1F).

After HCT, NK immunophenotype and cytotoxic functions were fully restored, including normalization of the pre-HCT expanded subset of NK-like CD8+ T cells (Fig. 3A and 3B). This largely expanded subset may have resulted from an ineffective compensatory expansion of CD8+ T cells carrying the wild-type *IL2RG* allele to provide innate NK-specific cytotoxic functions. The T-cell responses against the HPV-16 E6 antigen remained stable before and after HCT, whereas the T-cell responses against L1 capsid antigens, representing preventive rather than therapeutic potential effects,[10] reflected a robust reactivity to immunization against HPV (with Gardasil 9 vaccine) in the bone marrow donor as well as in the case patient after HCT (Figs. S13 and S14). As observed previously,[11] interleukin-2 signaling and its biologic effects are modest in monocytes; nevertheless, a partial restoration of the immunoregulatory signaling of interleukin-4, another cytokine that signals through the common cytokine receptor γ-chain, was observed after HCT (Figs. S15 and S16). The shotgun metagenomic analysis of the skin microbiome after HCT showed a conspicuous reduction in the viral predominance, including a distribution of commensal α-, β-, and γ-HPV genera similar to those seen in healthy persons (Fig. 3C and 3D and Fig. S17).

DISCUSSION

The somatic reversion of *IL2RG* germline pathogenic variants has been documented previously.[12–14] However, in contrast with previously reported cases, our index patient had exclusively viral clinical manifestations, with an episode of HSV encephalitis in adolescence and recalcitrant cutaneous verruca and recurrent HPV-16–related nasal squamous-cell carcinoma as a young adult. Although revertant T cells and the compensatory expansion of NK-like CD8+ T cells on antigen exposure may have partially mitigated the clinical and immunologic phenotype, the persistence of V64A in NK cells and the functional implication of that persistence in the control and distribution of commensal HPVs were remarkable. Commensal HPVs are represented mostly by β-HPV in immunocompetent hosts. However, the expansion of α-HPV,[4] including high-risk HPV variants associated with severe dysplasia and squamous-cell carcinoma in humans that are transmitted by self-inoculation or sexual contact, suggests that effective control of HPVs in general and specific HPV genera in particular requires intertwined innate and adaptive immunologic functions. In our case patient, we found that these immunologic functions were coordinated by the γ-chain family of cytokines and may involve antigen-presenting and adaptive cytotoxic functions but also innate NK-mediated cytotoxic functions. The specific defect in NK development and cytotoxic function caused by the germline V64A variant, in addition to the somatic mosaicism reverting such defect in the T-cell lineage, generated a unique clinical and immunologic phenotype that revealed the different roles of effector functions of T cells,

myeloid cells, and NK cells in the control of HPV colonization and immunopathogenesis. Although isolated inborn NK-cell deficiencies are rare and complex, genetic predisposing factors to HPV-related diseases have been suggested. This case underscores the critical role for NK cells in human host defense and, more specifically, in the susceptibility and prognosis of HPV-related diseases.[15–17]

The outcomes of HPV-related diseases after HCT in infancy for severe combined immunodeficiency are inconsistent, and recurrent or refractory HPV-related diseases despite HCT have been reported in a substantial proportion of patients.[18,19] It is noteworthy that patients who have been evaluated to date have been heterogeneous with respect to myeloid chimerism, the type of HCT that was performed (i.e., conditioning, donor source, and approach to graft-versus-host prophylaxis), NK-cell and functional recovery, underlying genetic defects, possible γ-chain expression in keratinocytes, and the virologic and clinical characteristics of HPV infections.[20–22] Our findings suggest that a consistent recovery of both innate and adaptive immunologic functions, including adequate NK cytotoxic function in the context of myeloid and lymphoid chimerism, is required to contain HPV colonization after HCT to repair *IL2RG* defects.

In our case patient, the stable regression of verruca and HPV-16–related mucosal squamous-cell carcinoma along with the reduction of the skin virome indicates that improved control of HPV colonization and ensuing HPV disease is achievable. Although T cells, monocytes, and tissue-resident myeloid cells may all participate to control HPV-related disease under different clinical conditions, the consistency in E6 HPV-specific T-cell responses before and after HCT, as well as the modest effects of interleukin-2 signaling in monocytes after HCT, corroborate the primary role of NK cells in the control of HPV-related diseases in this patient. Notably, the decreased frequency of perforin-expressing and terminally mature (KIR+) NK cells, as well as the impaired interleukin-2 signaling, suggest that both the maturation and homeostasis of NK cells are affected by the loss of *IL2RG* function and can result in impaired cytotoxic function. In addition, the extent of skin and mucosal colonization by HPVs (especially α-HPV)[4] may represent a virologic precursor of HPV-mediated dysplastic changes and may facilitate the risk stratification of patients with HPV-related diseases and their response to immunologic therapies, instead of being a mere marker for the immunologic competence of a specific host.

Novel therapeutic approaches that combine local ablative strategies and immunologic interventions (including checkpoint inhibition[23]) that are aimed at enhancing adaptive and innate NK-mediated immunosurveillance coordinated by γ-chain cytokines may contribute to the prevention of high-grade dysplasia or malignant lesions and improve HPV-related clinical outcomes in both immunocompromised and immunocompetent hosts.

Supplementary Material

Refer to Web version on PubMed Central for supplementary material.

Acknowledgments

We thank Meera Patel, Ornella Sortino, and Sean Conlan for their technical support; Mark J. Parta for providing clinical care; Sergio Rosenzweig, Julie Niemela, and Jennifer Stoddard for performing targeted next-generation sequencing; Stefania Pittaluga for interpreting histologic findings; and the NIH HPC Biowulf Cluster for providing computational resources.

REFERENCES

1. Schiller JT, Castellsagué X, Villa LL, Hildesheim A. An update of prophylactic human papillomavirus L1 virus-like particle vaccine clinical trial results. Vaccine 2008;26:Suppl 10:K53–K61. [PubMed: 18847557]
2. Lei J, Ploner A, Elfström KM, et al. HPV vaccination and the risk of invasive cervical cancer. N Engl J Med 2020;383: 1340–8. [PubMed: 32997908]
3. Stevanović S, Helman SR, Wunderlich JR, et al. A phase II study of tumor-infiltrating lymphocyte therapy for human papillomavirus-associated epithelial cancers. Clin Cancer Res 2019;25:1486–93. [PubMed: 30518633]
4. Tirosh O, Conlan S, Deming C, et al. Expanded skin virome in DOCK8-deficient patients. Nat Med 2018;24:1815–21. [PubMed: 30397357]
5. Leiding JW, Holland SM. Warts and all: human papillomavirus in primary immunodeficiencies. J Allergy Clin Immunol 2012;130:1030–48. [PubMed: 23036745]
6. Noguchi M, Nakamura Y, Russell SM, et al. Interleukin-2 receptor gamma chain: a functional component of the interleukin-7 receptor. Science 1993;262:1877–80. [PubMed: 8266077]
7. Leonard WJ, Lin J-X, O'Shea JJ. The γ_c family of cytokines: basic biology to therapeutic ramifications. Immunity 2019;50: 832–50. [PubMed: 30995502]
8. Doorbar J, Egawa N, Griffin H, Kranjec C, Murakami I. Human papillomavirus molecular biology and disease association. Rev Med Virol 2015;25:Suppl 1:2–23. [PubMed: 25752814]
9. Dimitrova D, Gea-Banacloche J, Steinberg SM, et al. Prospective study of a novel, radiation-free, reduced-intensity bone marrow transplantation platform for primary immunodeficiency diseases. Biol Blood Marrow Transplant 2020;26: 94–106. [PubMed: 31493539]
10. Joura EA, Giuliano AR, Iversen O-E, et al. A 9-valent HPV vaccine against infection and intraepithelial neoplasia in women. N Engl J Med 2015;372:711–23. [PubMed: 25693011]
11. Varker KA, Kondadasula SV, Go MR, et al. Multiparametric flow cytometric analysis of signal transducer and activator? of transcription 5 phosphorylation in immune cell subsets in vitro and following interleukin-2 immunotherapy. Clin Cancer Res 2006;12:5850–8. [PubMed: 17020993]
12. Kuijpers TW, van Leeuwen EMM, Barendregt BH, et al. A reversion of an IL2RG mutation in combined immunodeficiency providing competitive advantage to the majority of CD8+ T cells. Haematologica 2013;98:1030–8. [PubMed: 23403317]
13. Hsu AP, Pittaluga S, Martinez B, et al. IL2RG reversion event in a common lymphoid progenitor leads to delayed diagnosis and milder phenotype. J Clin Immunol 2015:35:449–53. [PubMed: 26076747]
14. Okuno Y, Hoshino A, Muramatsu H, et al. Late-onset combined immunodeficiency with a novel IL2RG mutation and probable revertant somatic mosaicism. J Clin Immunol 2015;35:610–4. [PubMed: 26407811]
15. Mace EMM, Orange JS. Emerging insights into human health and NK cell biology from the study of NK cell deficiencies. Immunol Rev 2019;287:202–25. [PubMed: 30565241]
16. Espinoza JL, Nguyen VH, Ichimura H, et al. A functional polymorphism in the NKG2D gene modulates NK-cell cytotoxicity and is associated with susceptibility to human papilloma virus-related cancers. Sci Rep 2016;6:39231. [PubMed: 27995954]
17. Wagner S, Wittekindt C, Reuschenbach M, et al. CD56-positive lymphocyte infiltration in relation to human papillomavirus association and prognostic significance in oropharyngeal squamous cell carcinoma. Int J Cancer 2016;138:2263–73. [PubMed: 26662627]

18. Neven B, Leroy S, Decaluwe H, et al. Long-term outcome after hematopoietic stem cell transplantation of a single-center cohort of 90 patients with severe combined immunodeficiency. Blood 2009;113: 4114–24. [PubMed: 19168787]

19. Gaspar HB, Harwood C, Leigh I, Thrasher AJ. Severe cutaneous papillomavirus disease after haematopoietic stem-cell transplantation in patients with severe combined immunodeficiency. Br J Haematol 2004;127:232–3. [PubMed: 15461635]

20. Kamili QUA, Seeborg FO, Saxena K, et al. Severe cutaneous human papillomavirus infection associated with natural killer cell deficiency following stem cell transplantation for severe combined immunodeficiency. J Allergy Clin Immunol 2014;134(6):1451.e1–1453.e1. [PubMed: 25159470]

21. Laffort C, Le Deist F, Favre M, et al. Severe cutaneous papillomavirus disease after haemopoietic stem-cell transplantation in patients with severe combined immune deficiency caused by common gammac cytokine receptor subunit or JAK-3 deficiency. Lancet 2004;363:2051–4. [PubMed: 15207958]

22. Vély F, Barlogis V, Vallentin B, et al. Evidence of innate lymphoid cell redundancy in humans. Nat Immunol 2016;17: 1291–9. [PubMed: 27618553]

23. Porichis F, Hart MG, Massa A, et al. Immune checkpoint blockade restores HIV-specific CD4 T cell help for NK cells. J Immunol 2018;201:971–81. [PubMed: 29934472]

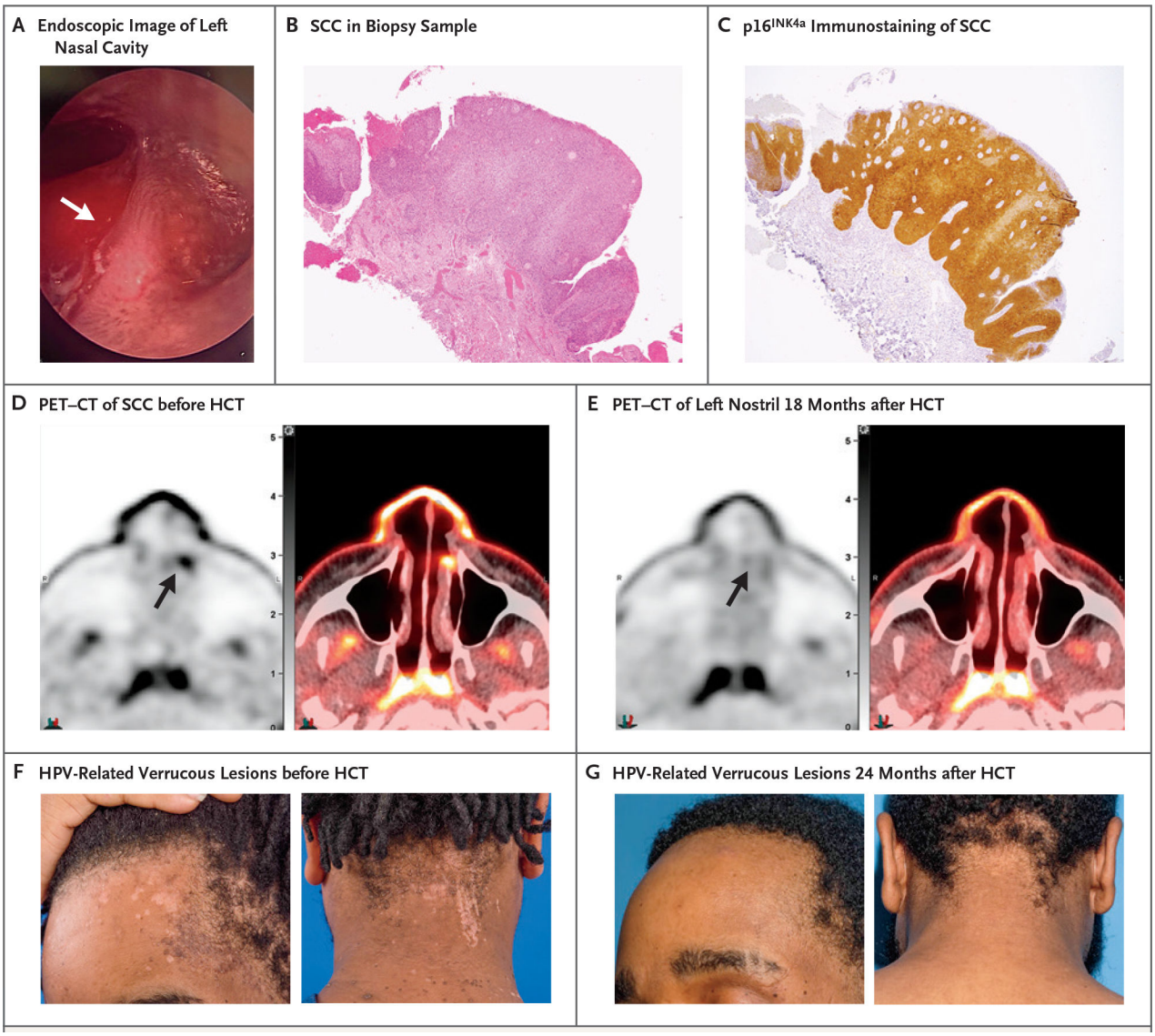

Figure 1. Clinical and Imaging Findings in the Case Patient with Recurrent Human Papillomavirus (HPV)–Related Diseases.

Panel A shows the results of fiberoptic endoscopic examination of the patient's left nasal cavity, where a sessile hyperkeratotic lesion was identified in the left nasal vestibule (white arrow). **Panel B** shows a thick epithelial layer with loss of stratification consistent with squamous-cell carcinoma (SCC) in situ in a biopsy sample of the hyperkeratotic lesion at the left inferior turbinate (hematoxylin and eosin staining). **Panel C** shows that the SCC in situ was strongly and diffusely positive for staining (indicated in brown) with antibody against $p16^{INK4a}$, a tumor-suppressor protein that is overexpressed in HPV-related cancers. **Panel D** shows the results of combined positron-emission tomography and computed tomography (PET–CT) with ^{18}F-fluorodeoxyglucose (18-FDG) indicating increased glucose metabolic activity in the left nasal vestibule (black arrow) before the patient underwent allogeneic hematopoietic-cell transplantation (HCT). **Panel E** shows the results of PET–CT 18 months after the patient underwent HCT, indicating resolution of abnormal metabolic activity in

the left nasal cavity. Physiologic 18-FDG uptake is noted in the nasopharynx (adenoids) and in the visualized portions of the temporalis muscles within the infratemporal fossae. **Panel F** shows flat warts (verruca plana) and scattered verruca vulgaris extending beyond the hairline on the patient's forehead and neck before HCT. **Panel G** shows resolution of these manifestations 24 months after HCT.

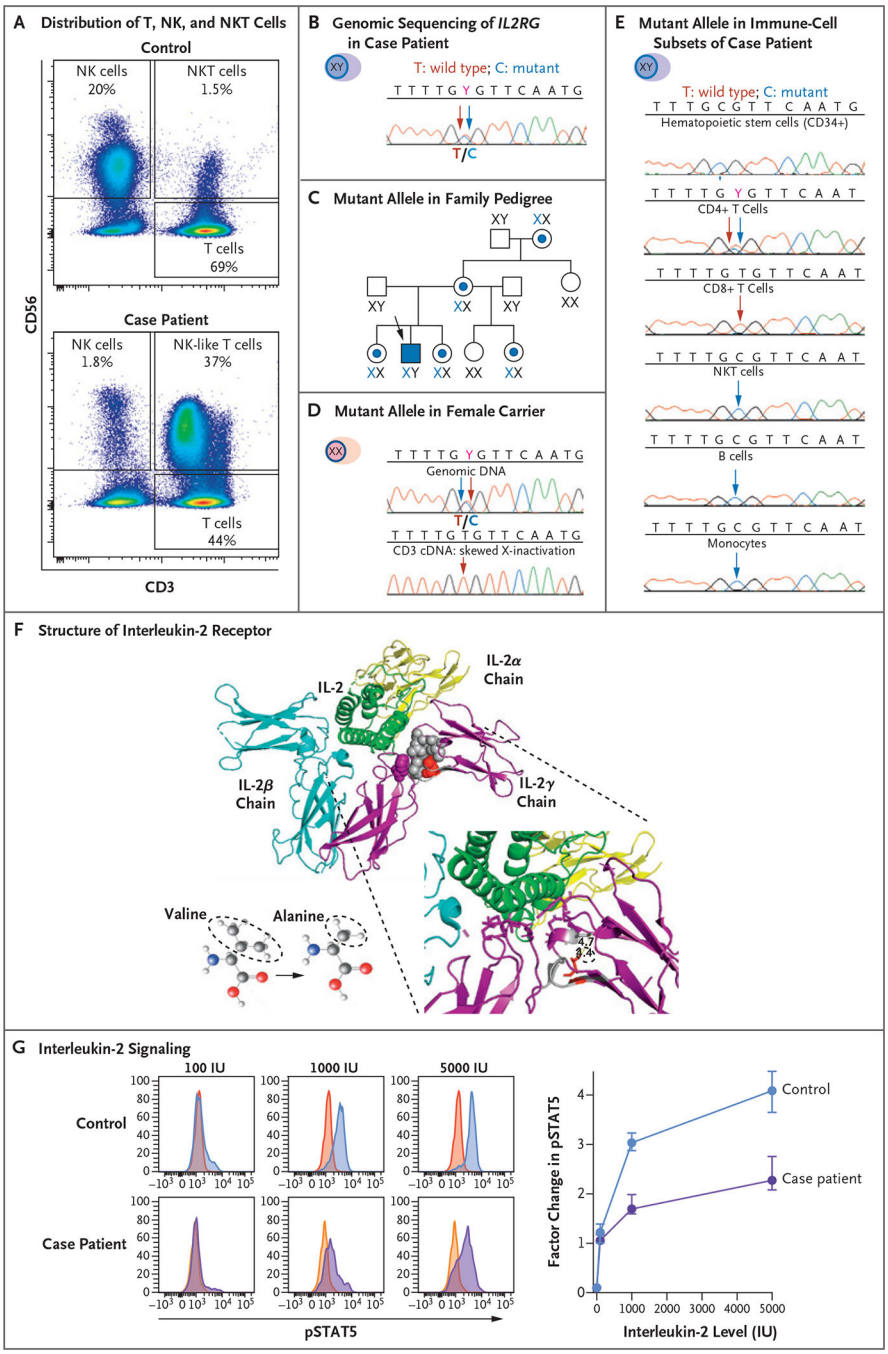

Figure 2. Genetic and Functional Analysis of the Common Cytokine Receptor γ-Chain.

Panel A shows flow cytometric analysis of the expression of CD56 and CD3 cells in peripheral-blood mononuclear cells (PBMCs) obtained from a healthy control (upper graph) and the case patient (lower graph). The analysis identifies subsets of natural killer (NK) cells and NK T (NKT) cells. The sample from the case patient shows an expansion of NK-like (CD3+CD56+) T cells and a reduced proportion of functional mature NK cells (CD3− $CD56^{dim}$). **Panel B** shows genomic sequencing of the X-linked gene interleukin-2 receptor subunit gamma (*IL2RG*) in DNA extracted from PBMCs obtained from the case

patient, which documents the equal distribution of the wild-type T allele (red arrow) and mutant C allele (blue arrow) at codon 191. **Panel C** shows the distribution of the *IL2RG* C allele with the c.191 mutation in the patient's family pedigree. A blue dot and X identify female carriers of the mutant allele, and the case patient is identified by a blue square. **Panel D** shows the distribution of the mutant *IL2RG* C allele in the genomic DNA (upper graph) and in the complementary DNA (cDNA) from sorted T cells (lower graph) obtained from a female carrier in the patient's family. Although both wild-type T alleles and mutant C alleles are present in genomic DNA from PBMCs, only the wild-type T allele appears in cDNA extracted from T cells. **Panel E** shows the distribution of the mutant *IL2RG* C allele in genomic DNA extracted from different cell subsets of the case patient. Somatic reversion of the mutated C allele appears only in CD4+ and CD8+ T cells. **Panel F** shows the heterotrimeric structure of the interleukin-2 receptor (IL-2R) in complex with interleukin-2 (IL-2, green ribbon). The three distinct and noncovalently linked IL-2Rα chain (yellow ribbon), IL-2Rβ chain (blue ribbon), and IL-2Rγ chain (purple ribbon) contribute to define the high-affinity IL-2 binding site. The side chain of p.64V (red spheres) in a compact hydrophobic core (gray spheres) interacting with p.227F (purple spheres) contributes to defining the IL-2 binding site. The missense variant p.V64A has a smaller side chain than the wild type. **Panel G** shows histograms (at left) that represent the distribution of fluorescence intensity of phosphorylated signal transducer and activator of transcription 5 (pSTAT5) after incubation of PBMCs obtained from a healthy control and from the case patient with different levels of IL-2. After gating in the subset of CD3-CD56^{dim} functionally mature NK cells, the red and yellow histograms (which overlap and appear orange in spots) on the left side of each graph display the pSTAT5 fluorescence intensity in unstimulated condition, whereas the blue and purple histograms on the right side display the increase in pSTAT5 fluorescence after stimulation with 100, 1000, and 5000 IU of IL-2 in a representative experiment. The graph (at right) presents the cumulative data of five independent experiments presented as the median and interquartile range of the factor change in the median fluorescence intensity of pSTAT5 between unstimulated and IL-2–stimulated conditions in the case patient and in healthy controls. The reduction in the pSTAT5 factor change is consistent with reduced IL-2 signaling in the case patient as compared with two healthy controls.

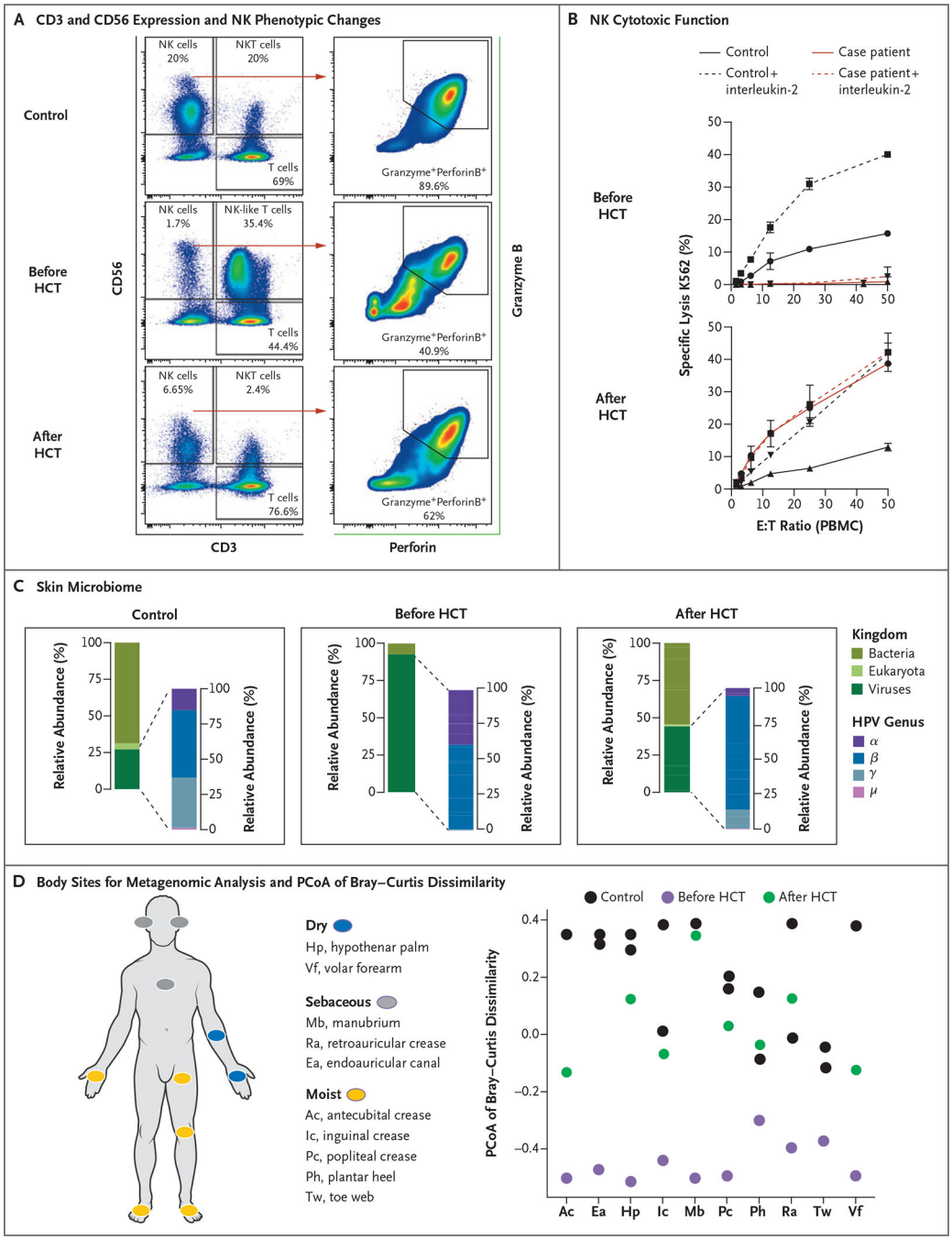

Figure 3. Changes in NK Cytotoxic Function and Skin Microbiome after Hematopoietic-Cell Transplantation.

Panel A shows flow cytometric analysis of the expression of CD56 and CD3 in PBMCs obtained from a healthy control (upper graph) and the case patient (middle and lower graphs), along with the distribution of NK and NK-like T cells before and 24 months after the case patient underwent HCT. In the graphs at right, the expression of granzyme B and perforin in CD3+CD56+ NK cells is presented in a healthy control and in the case patient before and after HCT. After HCT, the distribution of functional mature NK

cells (CD3−CD56^{dim}) and NK-like T cells is normalized, along with the proportion of NK cells coexpressing both granzyme B and perforin. **Panel B** shows the evaluation of NK cytotoxicity by a 4-hour chromium-51 release assay in the presence of 1000 U per milliliter of interleukin-2 (dashed line) or the absence of interleukin-2 (solid line). PBMCs from the case patient before and 24 months after HCT (red) or a healthy control (black) were used as effectors (E) against K562 target (T) cells at indicated ratios in three replicates per experimental condition. **Panel C** shows skin shotgun metagenomics data presented as the mean relative abundance of total mapped microbial reads (normalized to genome length) averaged across at most 10 body sites per person per time point. Two healthy controls were compared with the case patient for whom samples had been collected before and 24 months after HCT. The graphs at left present the mean relative abundance of the skin microbiome classified at the kingdom level (Eukaryota, Bacteria, and Virus), with viruses broken down into members of the *Papillomaviridae* genera as compared with all other viruses, including other eukaryotic viruses and viruses in bacteria. In the graphs at right, the mean relative abundance of four HPV genera (α, β, γ, and μ) on the skin is presented. **Panel D** shows the distribution of the 10 body sites sampled for the skin shotgun metagenomic analysis and principal coordinates analysis (PCoA) of Bray–Curtis dissimilarity. The first PCoA axis, which explained 28% of the variation in the data, is plotted as a function of body site. Each point represents a sample. Shapes and colors indicate whether samples were collected from healthy controls or from the case patient before or 24 months after HCT.